Article

SOURCE DATA | TRANSPARENT PROCESS

THE EMBO JOURNAL

The miR-379/miR-410 cluster at the imprinted *Dlk1-Dio3* domain controls neonatal metabolic adaptation

Stéphane Labialle[1,2,†], Virginie Marty[1,2,†], Marie-Line Bortolin-Cavaillé[1,2], Magali Hoareau-Osman[1,2], Jean-Philippe Pradère[3,4], Philippe Valet[3,4], Pascal GP Martin[1,2,5,6] & Jérôme Cavaillé[1,2,*]

Abstract

In mammals, birth entails complex metabolic adjustments essential for neonatal survival. Using a mouse knockout model, we identify crucial biological roles for the miR-379/miR-410 cluster within the imprinted *Dlk1-Dio3* region during this metabolic transition. The miR-379/miR-410 locus, also named C14MC in humans, is the largest known placental mammal-specific miRNA cluster, whose 39 miRNA genes are expressed only from the maternal allele. We found that heterozygote pups with a maternal—but not paternal—deletion of the miRNA cluster display partially penetrant neonatal lethality with defects in the maintenance of energy homeostasis. This maladaptive metabolic response is caused, at least in part, by profound changes in the activation of the neonatal hepatic gene expression program, pointing to as yet unidentified regulatory pathways that govern this crucial metabolic transition in the newborn's liver. Not only does our study highlight the physiological importance of miRNA genes that recently evolved in placental mammal lineages but it also unveils additional layers of RNA-mediated gene regulation at the *Dlk1-Dio3* domain that impose parent-of-origin effects on metabolic control at birth and have likely contributed to mammal evolution.

Keywords epigenetic; genomic imprinting; metabolic adaptation; microRNA; mouse model

Subject Categories Development & Differentiation; Metabolism; RNA Biology

DOI 10.15252/embj.201387038 | Received 30 September 2013 | Revised 2 July 2014 | Accepted 7 July 2014 | Published online 14 August 2014

The EMBO Journal (2014) 33: 2216–2230

Introduction

MicroRNAs (miRNAs) are endogenously expressed, ~19–23 nt-long non-coding RNAs (ncRNA) that silence gene expression at the post-transcriptional level, mostly via imperfect base-pairing interactions that occur preferentially within the 3′ untranslated regions (UTRs) of target mRNAs (Fabian & Sonenberg, 2012). Through their ability to target hundreds, perhaps even thousands of mRNAs, miRNAs are now considered as potent post-transcriptional regulators in an ever-growing list of developmental, physiological, or pathological contexts (Bushati & Cohen, 2007). Most conclusions drawn so far for mammalian miRNAs rely on computational mRNA target predictions coupled to gain- or loss-of-function approaches conducted mostly *in vitro* using cellular models. Although informative, these approaches do not undisputedly demonstrate the physiological significance of miRNAs. In that context, most miRNA knockout (KO) mice described so far do not exhibit overt abnormalities under classical mouse husbandry conditions, although defects can become apparent in physiologically challenging contexts (Leung & Sharp, 2010; Mendell & Olson, 2012). Accordingly, we still need to determine precisely, at the whole-organism level, the extent to which defects in miRNA-mediated regulation yield clear and interpretable phenotypic consequences (Park *et al*, 2010, 2012).

In mammals, a subset of poorly conserved miRNA genes is subjected to genomic imprinting, a developmentally regulated form of epigenetic regulation that causes mono-allelic expression in a parent-of-origin dependent manner. That is, for a given gene, only one of the two parental alleles is transcriptionally competent (Barlow & Bartolomei, 2014). Most imprinted miRNA genes identified so far are organized as large (~40–100 kb) non-protein-coding transcriptional arrays that generate a large number (~50–100) of RNA species of related sequences. These clustered, tandemly repeated miRNAs likely arose through segmental duplication followed by sequence diversification and are presumably co-expressed as, and processed from, a single (or a few) long primary non-coding transcript(s). Remarkably, this unusual mode of genomic organization and epigenetic regulation appears specific to imprinted loci (Labialle & Cavaille, 2011) and has been reported at

1 Laboratoire de Biologie Moléculaire Eucaryote, UPS, Université de Toulouse, Toulouse, France
2 CNRS, LBME, UMR5099, Toulouse, France
3 Institut National de la Santé et de la Recherche Médicale (INSERM), U1048, Toulouse, France
4 Institut des Maladies Métaboliques et Cardiovasculaires (I2MC), Université de Toulouse, Université Paul Sabatier, Toulouse, France
5 INRA, UMR1331, TOXALIM (Research Centre in Food Toxicology), Toulouse, France
6 Université de Toulouse, INP, UPS, TOXALIM, Toulouse, France
*Corresponding author. Tel: +33 561335934; Fax: +33 561335886; E-mail: cavaille@ibcg.biotoul.fr
†These authors contributed equally to this work

three evolutionarily distinct chromosomal regions: the eutherian-specific *Dlk1-Dio3* domain (Seitz *et al*, 2003), the primate-specific C19MC region (Noguer-Dance *et al*, 2010), and the rodent-specific *Sfmbt2* cluster (Wang *et al*, 2011).

The ~1-Mbp eutherian-specific imprinted *Dlk1-Dio3* chromosomal region on distal mouse chromosome 12 (orthologous to human chromosome 14q32) expresses three paternally expressed protein-coding genes (*Dlk1*, *Rtl1*, and *Dio3*) and several maternally expressed non-protein-coding transcripts, including *Gtl2* as well as numerous box C/D small nucleolar (sno) RNAs and miRNAs (da Rocha *et al*, 2008) (Fig 1A). Many of these small RNAs are embedded within, and processed from, introns of poorly characterized long ncRNAs: In the mouse, many snoRNAs and miRNAs are intron-encoded within transcripts called *Rian* and *Mirg*, respectively. Most miRNA genes are grouped into two main regions, the miR-127/miR-136 cluster originating from an anti-*Rtl1* transcript and the

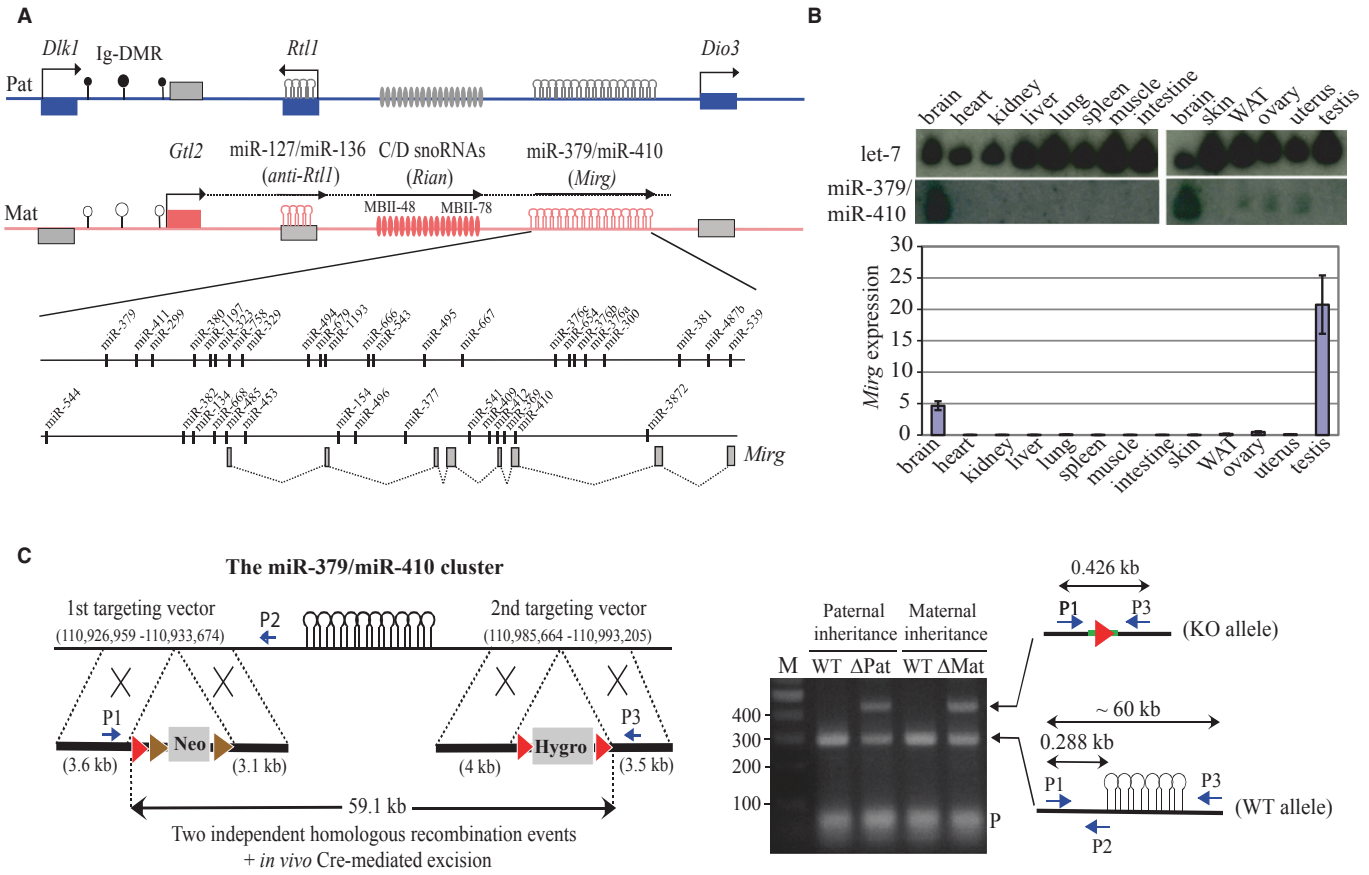

Figure 1. Targeted deletion of the miR-379/miR-410 cluster at the imprinted *Dlk1-Dio3* domain.

A Schematic representation of the ~1-Mbp imprinted *Dlk1-Dio3* region on mouse distal chromosome 12. Paternally expressed protein-coding genes (*Dlk1*, *Rtl1*, and *Dio3*) are symbolized by blue rectangles, while maternally expressed miRNA and C/D snoRNA genes are depicted by pink stem loops and ovals, respectively. *Gtl2* (pink rectangle) is a long, maternally expressed non-coding RNA (ncRNA) gene. *Anti-Rtl1*, *Rian*, and *Mirg* correspond to poorly characterized maternally expressed ncRNAs from which some, but not all, miRNAs and C/D snoRNAs are processed. It should be noted, however, that some deposited RNA sequences may simply represent RNA species whose functionality, if any, remains questionable (Chiang *et al*, 2010). Arrows indicate the sense of transcription, with the horizontal broken line highlighting the notion that *Gtl2*, *anti-Rtl1*, *Rian*, and *Mirg* may belong to the same transcription unit. Differentially methylated regions, including the imprinting center (Ig-DMR) that controls imprinted expression over the domain, are indicated by filled and open lollipops (methylated and un-methylated, respectively). The relative positions of hairpin-like (pre-miRNA) structures within the miR-379/miR-410 cluster are indicated in the enlarged inset. Note that most pre-miRNA genes at the 3′ end of the cluster are positioned within introns of *Mirg* (gray rectangles and dotted lines represent exons and splicing events, respectively).

B Top: The tissue-specific expression pattern of miRNAs was assayed by Northern blot analysis of adult mouse tissues as indicated on the panel, using a mixture of ^{32}P-labelled oligonucleotides antisense to some miRNAs scattered along the cluster (miR-411, 323, 376b, 376a, 134, 154, and 410). The same membrane was probed with a *let-7* oligo probe (gel loading control). Bottom: The tissue-specific expression pattern of *Mirg* host gene transcripts was assayed by RT–qPCR relative to *Gapdh* using the same set of tissues. Note that *Mirg* expression, but not that of miRNAs, is detected in testes, indicating that post-transcriptional regulation may occur in this tissue. WAT: white adipose tissue. Data are expressed as mean ± s.e.m.

C Cre/loxP-mediated site-specific deletion of the miR-379/miR-410 cluster. Left: Targeting strategy for disrupting the miR-379/miR-410 cluster through two independent homologous recombination events. Genome coordinates: UCSC Genome Browser, mouse, NCB137/mm9. Red and brown arrows indicate loxP and FRT recognition sites for the Cre and Flp site-specific recombinases, respectively. Right: PCR confirmation of the deletion using appropriate P1, P2, and P3 primers. The sequence of the deleted region was further confirmed by DNA sequencing. ΔMat and ΔPat represent heterozygous individuals with maternally and paternally inherited deletions, respectively, while WT correspond to wild-type littermate controls. M: DNA ladder (bp).

Source data are available online for this figure.

miR-379/miR-410 cluster (also referred to as C14MC in human). A few more are found scattered along the *Dlk1-Dio3* region. The miR-127/miR-136 cluster silences the paternally expressed *Rtl1* mRNAs through siRNA-like mechanisms (Seitz *et al*, 2003; Davis *et al*, 2005), and this *trans*-allelic RNAi-mediated regulation plays critical roles in placental development (Sekita *et al*, 2008). Although numerous functions for the miR-379/miR-410 cluster have been inferred from aberrant expression in pathological contexts or from enforced or knockdown expression experiments performed *in vitro* (Labialle & Cavaille, 2011; Benetatos *et al*, 2012; Girardot *et al*, 2012), the biological importance of this large miRNA cluster remains elusive. Of note, several studies have pointed out regulatory roles in neuronal functions, especially for miR-134 (Schratt *et al*, 2006; Fiore *et al*, 2009; Christensen *et al*, 2010; Gao *et al*, 2010; Jimenez-Mateos *et al*, 2012; Bicker *et al*, 2013; Rago *et al*, 2014). A correct dosage of imprinted genes encoded at the mouse *Dlk1-Dio3* genomic interval is essential for embryonic growth and postnatal survival, as well as for muscle, skeletal, placental, and neuronal development (da Rocha *et al*, 2008). The functional significance of the corresponding imprinted human genes at 14q32 is supported by human syndromes of respiratory insufficiency, altered thoracic development, mental retardation, obesity, growth retardation, and precocious puberty (Kagami *et al*, 2008). The *Dlk1-Dio3* genomic interval has also been linked genetically to diabetes (Wallace *et al*, 2010; Kameswaran *et al*, 2014). Whether the miR-379/miR-410 (C14MC) cluster contributes to one (or several) of these physiological processes or pathological contexts remains an open question.

Newly available epigenetically regulated arrays of miRNA genes raise intriguing questions regarding the evolutionarily meaning of their repeated structures in relation to their mono-allelic expression patterns and the potential redundancy or divergence in the functions of related miRNA genes within a given cluster (Labialle *et al*, 2011). Studying these imprinted arrays of miRNA genes therefore provides unique opportunities to address the physiological roles of lineage-specific miRNAs, but also to evaluate how a large number of coordinately expressed miRNAs can impact gene regulatory networks. To elucidate the biological roles of the large miR-379/miR-410 cluster at the *Dlk1-Dio3* domain, we have used a constitutive mouse KO model. Unexpectedly, a subset of miR-379/miR-410-deficient neonates failed to maintain energy homeostasis and die shortly after birth. These neonatal metabolic deficiencies—affecting both lipid and glucose metabolism—are very likely caused, at least in part, by defects in the temporal activation of a large set of metabolic genes in the newborn's liver. This is, to the best of our knowledge, the first demonstration that miRNAs exert critical functions at the transition from fetal to postnatal life in mammals.

Results

Targeted disruption of the miR-379/miR-410 cluster

The imprinted *Dlk1-Dio3* domain contains the largest eutherian-specific miRNA cluster: The miR-379/miR-410 cluster (Fig 1A), named C14MC in humans, believed to produce 77 and 63 mature miRNAs in the mouse and humans, respectively (http://www.mirbase.org/). In the adult mouse, miR-379/miR-410 expression is mostly restricted to the brain (Fig 1B). In contrast, during development and also at birth, these miRNAs are widely expressed in many non-brain tissues (Fig 2A–C, and Supplementary Fig S4). To assess the biological functions of miR-379/miR-410 *in vivo*, we created a constitutive KO mouse model carrying a Cre/loxP-mediated ~59-kb-long deletion (Fig 1C) that removes the entire miRNA cluster (denoted as ΔmiR).

The miR-379/miR-410 cluster is regulated by genomic imprinting; only the maternally inherited allele is competent for transcription (Seitz *et al*, 2003). Accordingly, we analyzed ΔmiR mice generated by two types of crosses: (i) wild-type females with heterozygous males (paternal inheritance of the targeted deletion) and (ii) wild-type males with heterozygous females (maternal inheritance of the targeted deletion). These two reciprocal crosses are expected to generate 50% wild-type and 50% heterozygous animals. In principle, only heterozygotes having inherited the deletion from their mother (denoted as ΔMat) are deficient for miR-379/miR-410 expression. In contrast, heterozygotes having inherited the deletion from their father (denoted as ΔPat) express the miRNA cluster normally. We therefore analyzed ΔMat and ΔPat animals since these two classes of heterozygotes are genetically comparable, thus alleviating any potential confounding effects due to differences in genetic background. Wild-type littermates (denoted as WT) were also used as controls.

We first validated our KO model by demonstrating that, as expected, upon maternal but not paternal inheritance, the targeted miRNA genes were no longer expressed in embryo (E18.5), placenta (E18.5), and adult brain (Fig 2A). More sensitive RT–qPCR experiments revealed very weak, but still detectable, expression for some individual miRNAs (Fig 2C) or for the *Mirg* host gene in the embryo (Fig 2D), indicating that leaky expression (~5%) can occur on the normally silenced paternal allele in some tissues. More importantly, the level of expression of the surrounding imprinted ncRNA and protein-coding genes (Fig 2D), as well as their imprinted status (Supplementary Fig S1), remained unaffected, making it very unlikely that ΔmiR removes important regulatory elements that govern imprinted expression over the *Dlk1-Dio3* genomic interval.

Genetic ablation of the miR-379/miR-410 cluster leads to partially penetrant neonatal lethality

After extensive breeding in the C57BL/6J genetic background, we found that, upon maternal but not paternal inheritance, ~39% of ΔMat animals were missing at 3–4 weeks of age (Table 1). This alteration in the Mendelian ratio was likewise observed in crosses where the dams inherited the deletion paternally or maternally, thus excluding any grand-parental effects (Table 2). ΔmiR does not lead to embryonic lethality since ΔMat concepti reached late gestation (E18.5) at the expected Mendelian frequencies (Table 1) without any obvious alteration in overall growth of the embryos or placenta (Supplementary Fig S2). ΔMat pups were born alive, but half of them died within ~15–40 h post-delivery (Table 3). Maternal care was normal as were the weights and overall appearance of major neonatal organs we examined (Supplementary Fig S2). Once neonates overcame the fetal-to-postnatal transition, survivors did not exhibit any significant increase in lethality over at least 8 months. However, upon maternal, but not paternal, inheritance, both males and females were transiently growth-retarded ~3 weeks after birth, coinciding with the suckling–weaning transition (Supplementary Fig S2).

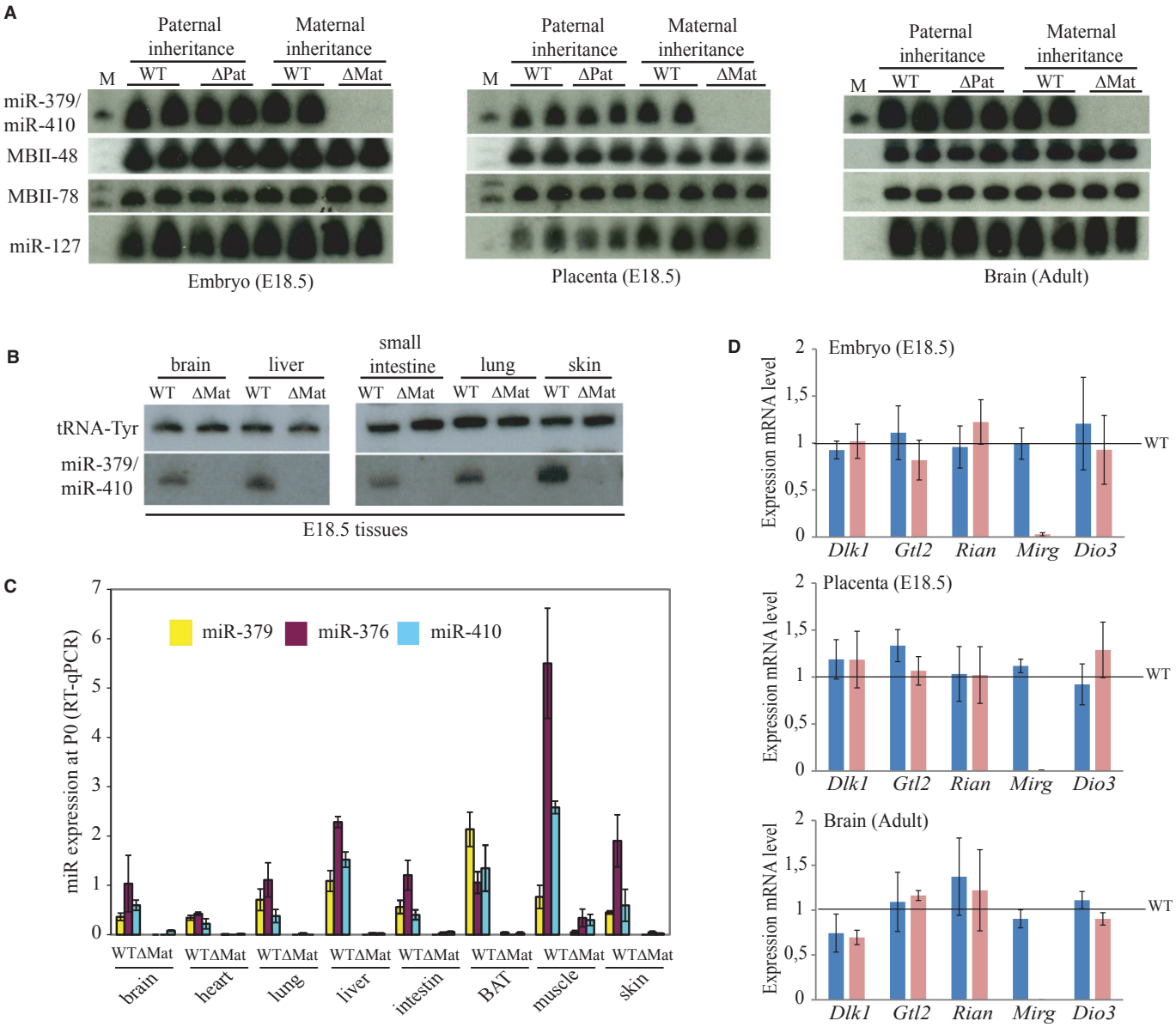

Figure 2. Targeted deletion of the miR-379/miR-410 cluster does not affect the expression levels of flanking genes.

A Expression of the miR-379/miR-410 cluster and its flanking C/D snoRNA (MBII-78, MBII-48) and miRNA (miR-127) genes was assayed by Northern blot analysis of the indicated samples (two individuals per genotype).

B Expression of the miR-379/miR-410 cluster was assayed by Northern blot analysis of the dissected tissues indicated above the panels from WT or ΔMat E18.5 embryos. A tRNA-specific probe was used as the internal loading control.

C Expression of selected miRNAs (miR-379, miR-376a, and miR-410) was assayed by RT–qPCR relative to U6 snRNA in P0 tissues prepared from WT or ΔMat individuals (n = 3 per genotype), as indicated below the histograms. BAT: brown adipose tissue. Data are expressed as mean ± s.e.m.

D Expression of mRNAs (*Dlk1* and *Dio3*) and mRNA-like transcripts (*Gtl2*, *Rian*, *Mirg*) was assayed by RT–qPCR relative to *Gapdh* mRNA in the indicated tissues. Blue and pink bars represent expression levels in ΔPat and ΔMat individuals, respectively (six individuals per genotype). Expression levels of WT were arbitrarily set to 1.

Source data are available online for this figure.

Genetic ablation of the miR-379/miR-410 cluster results in impaired neonatal glucose homeostasis

Neonatal death can result from a large spectrum of physiological defects (Turgeon & Meloche, 2009). In the absence of any apparent morphological defects and due to the timing of lethality, we hypothesized that ΔMat neonates may have deficiencies in maintaining energy homeostasis. Indeed, birth entails major metabolic challenges as the energy supply provided mostly as glucose by placental nutrition suddenly ceases. To combat this naturally occurring starvation episode, neonates first degrade their hepatic glycogen store constituted during late embryogenesis (glycogenolysis) and then activate gluconeogenesis, which is not active in the immediate postnatal period (Girard *et al*, 1992). As shown in

Table 1. Maternally, but not paternally inherited ΔmiR, leads to altered Mendelian ratios 4 weeks after birth but not before birth (E18.5).

	4-week-old mice		E18.5 embryos	
C57BL/6J (N6–N12)	Maternal inheritance	Paternal inheritance	Maternal inheritance	Paternal inheritance
Total individuals	753	656	65	54
Litter (*n*)	148	108	11	8
Sex				
Males	378	306	n.d.	n.d.
Females	375	350	n.d	n.d.
Observed genotypes				
WT	468	346	33	27
Heterozygotes	285	310	32	27
P-values	2.57e−11	0.16	0.9	1.0

Table 2. The altered Mendelian ratio 4 weeks after birth is not caused by the lack of expression of the miR-379/miR-410 cluster in the dams.

	Parental origin of ΔmiR in the dams	
	Paternal (miRNA expression)	Maternal (no miRNA expression)
Total individuals	472	281
Litter (*n*)	92	56
Sex		
Males	247	131
Females	225	150
Observed genotypes		
WT	298	170
ΔMat	174	111
P-values	1.14e−8	4.32e−4

Table 3. ΔMat neonates are born alive but die within 15–40 h after birth.

	Neonates (P0–P3)		
	Maternal inheritance		
Total individuals	93		
Litter (*n*)	14		
Time after birth	0–14 h	15–40 h	41–96 h
Observed genotypes			
WT	39 (6)	36 (3)	36 (0)
ΔMat	43 (5)	22 (21)	20 (2)
P-values	0.76	0.0002	n.d.

Numbers in parentheses represent dead pups, and *P*-values estimate the significance of the unequal number of dead pups in each genotype by the χ^2 test.

Fig 3A, blood glucose levels at P0 were reduced by ~20% in ΔMat neonates relative to WT littermates while, as expected, blood sugar concentration in ΔPat neonates was in the normal range. Interestingly, the distribution of glycemic status at P1 revealed that a subset of ΔMat neonates displayed severe hypoglycemia (defined here arbitrarily as glucose levels < 30 mg/dl) while glucose levels in the remaining mutants were only slightly lower than those of WT (Fig 3A and Supplementary Fig S3). A careful tracking showed that mutant dead pups collected between P0 and P1 together with profoundly hypoglycemic individuals at P1 account for 37.7% of ΔMat individuals (n = 17 litters, Table 4). Given the neonatal death observed around birth (Table 3) and the deficit of ΔMat individuals at weaning (Table 1), most of these severely hypoglycemic mutants are unlikely to survive the perinatal period, thus implying that hypoglycemia contributes to neonatal death. To challenge this assumption, WT and ΔMat neonates were systematically given subcutaneous glucose injections (50 µl, 10%) shortly after birth and then 4–6 h later (n = 10 litters). In order to avoid any bias due to the incomplete penetrance of the lethality, we only considered litters without any dead pups at the time of the first injections. As reported in Fig 3G, glucose injections rescued, at least in part, the neonatal lethality phenotypes since 25/31 (80.6%) glucose-injected mutants survived birth transition, with 24/25 still alive after weaning. In comparison, the perinatal survival rate of ΔMat without glucose injections was 42% (Table 3). We next sought to further appreciate the contribution of deficiencies in glucose homeostasis by studying pups kept separated from their mother and maintained in a moist, warm (32–35°C) atmosphere. This procedure alleviates confounding variables in that external sources of glucose cannot be provided by mother's milk. In a first pilot experiment during which we monitored continuously the fate of neonates, no ΔMat (0/10) neonates survived starvation over a 10-h period while 60% of WT (11/18) were still alive over the same time course (n = 4 litters; Fig 3H, left). In a second set of experiments, we asked whether glucose injections may extend the lifespan of ΔMat pups in such challenging metabolic environment. For each litter, half of the pups were injected subcutaneously with glucose, immediately after birth and then every 6 h over a period of 12 h. The remaining 50% of pups were injected with NaCl (50 µl, 0.9%) and used as controls (n = 5 litters). As shown in Fig 3H (right), lethality of ΔMat neonates could be delayed since 7/7 (100%) mutants and 5/7 (71%) WT pups injected with glucose survived up to 17 h. In comparison, all NaCl-injected control individuals were dead 17 h post-injection. The survival of 6/7 NaCl-injected ΔMat neonates at t + 10 h reflects probably the notion that hydration of pups contributes to their survival when no access to mother's milk is allowed. Altogether, these glucose rescue

Table 4. The neonatal fate of WT and ΔMat pups between P0 and P1

	Maternal inheritance (n = 17 litters)	
	ΔMat (n = 69)	WT (n = 61)
Dead pups (P0–P1)	17	6
Hypoglycemic pups (P1) (glycemic status < 30 mg/dl)	9	2
Dead + hypoglycemic pups (%)	37.7	13.1

experiments demonstrate that dysregulation of glycemia is a major early event linked to the neonatal lethality.

Genetic ablation of miR-379/miR-410 cluster alters neonatal glycogenolysis and gluconeogenesis

Because mobilization of glycogen stores is one of the very first metabolic adaptive events, we assessed hepatic glycogen levels. As shown in Fig 3C, ΔMat neonates at P0 had 40–50% higher

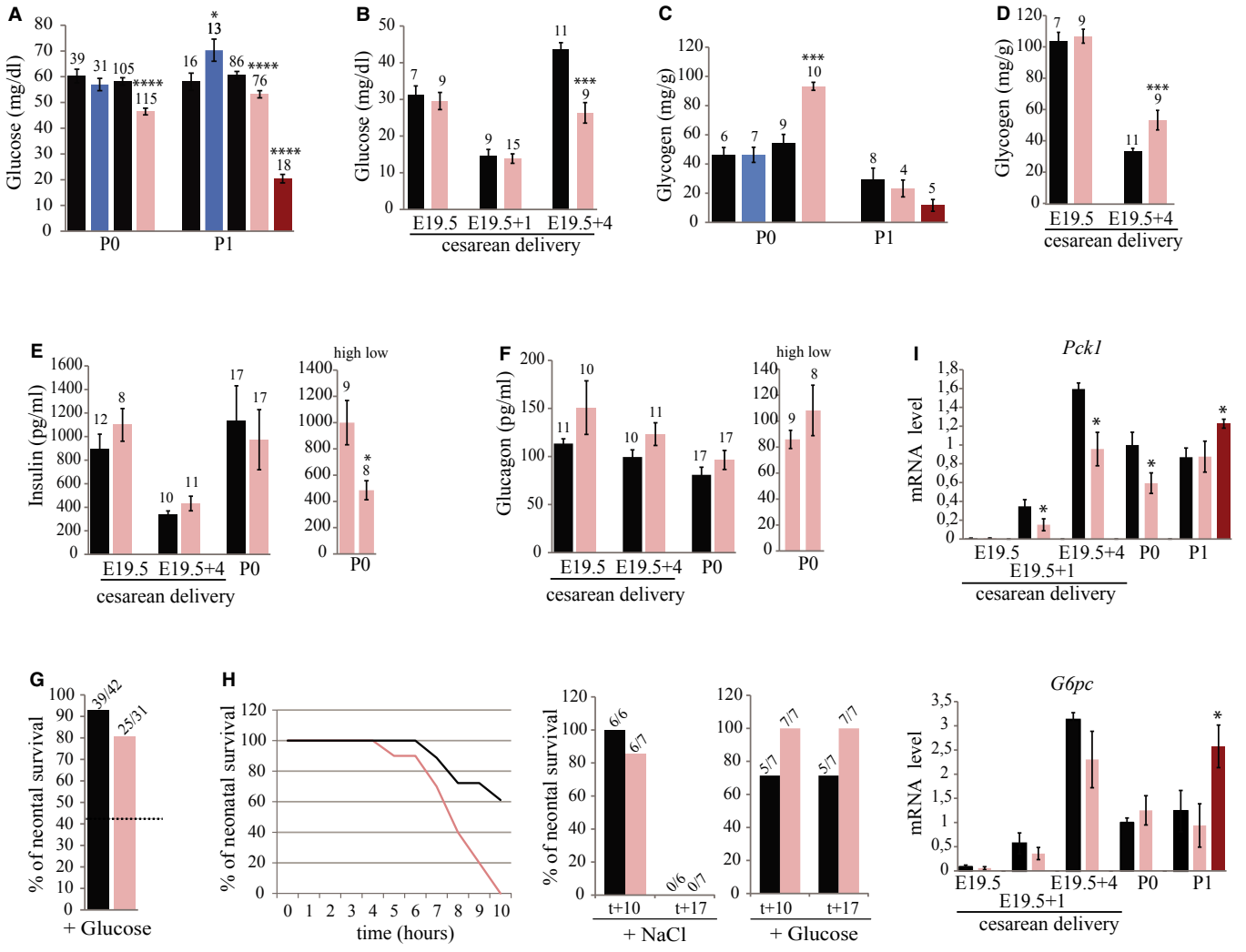

Figure 3. Maternal, but not paternal, deletion of the miR-379/miR-410 cluster impairs hepatic glycogenolysis and gluconeogenesis.

A–F Serum glucose (A, B), hepatic glycogen (C, D), insulin (E), glucagon (F) levels in WT (black), ΔMat (pink), severely hypoglycemic ΔMat (dark pink) or ΔPat (blue) neonates were measured in vaginally delivered neonates (P0, P1) or after cesarean delivery (E19.5, E19.5 + 1, E19.5 + 4). Insulin and glucagon levels of ΔMat individuals in the same cohort with the highest and lowest glucose concentration, denoted as high (50.78 ± 1.42 mg/dl) and low (27.38 ± 3.72 mg/dl), respectively, are also shown in the histograms to the right (E and F). Numbers of individuals analyzed are indicated above the histograms.

G Glucose injections rescue the neonatal lethality phenotype. Dotted lines represent the % of ΔMat neonatal survival as observed from dead pups collected perinatally (Table 3).

H Left: The lifespan of ΔMat neonates (pink line) is reduced relative to WT (black line) when P0 neonates were kept separated from their mother. Right: Glucose injections extend the lifespan of ΔMat neonates. Histograms show the survival rate of NaCl- or glucose-injected pups at 10 and 17 h post-injection.

I The temporal expression of the gluconeogenic *Pck1* and *G6pc* genes in liver (relative to *Gapdh*) was assayed by RT–qPCR (6 individuals per genotype).

Data information: Data are expressed as mean ± s.e.m.

hepatic glycogen contents than their WT littermates whereas, as expected, hepatic glycogen stores were in the normal range in ΔPat neonates. Given that glycogen appeared to be normally degraded in mutant neonates at P1 regardless of their glycemic status, we conclude that ΔMat neonates degrade glycogen at lower rates. To verify this hypothesis, serum glucose and hepatic glycogen levels were measured in embryos delivered by cesarean sections at embryonic day 19.5 (E19.5). Serum glucose levels and glycogen were measured one and four hours after embryo harvest (denoted hereafter as E19.5 + 1 and E19.5 + 4, respectively). As shown in Fig 3B and D, ΔMat neonates at E19.5 had glucose and glycogen levels similar to WT, excluding any deficiencies in trans-placental transfer of glucose and/or exacerbated accumulation of hepatic glycogen. As expected, both WT and ΔMat neonates displayed lower levels of glucose at E19.5 + 1. However, ΔMat neonates were deficient in glucose production since they failed to reach blood glucose levels comparable to WT at E19.5 + 4 (Fig 3B). Interestingly, over the same time course, they did not degrade their hepatic glycogen efficiently (Fig 3D), thus corroborating our previous conclusions drawn from vaginally delivered pups: ΔMat neonates inefficiently mobilize their glycogen stores.

That some ΔMat neonates at P1 are severely hypoglycemic while their glycogen stores are fully exhausted also argues for defects in the proper initiation of gluconeogenesis during the immediate perinatal period. To confirm this assumption, we monitored expression of two key glucogenic factors whose expression is known to be transcriptionally activated at birth: phosphoenolpyruvate carboxykinase 1 (*Pck1*) and glucose-6-phosphatase (*G6pc*). Consistent with an activation of gluconeogenic pathways at birth, *Pck1* and *G6pc* mRNA levels were dramatically up-regulated in WT neonate livers between E19.5 and E19.5 + 4 (Fig 3I, top and bottom). However, the neonatal induction of *Pck1* was found to be partially defective in ΔMat pups, while expression of *G6pc* appeared normal, albeit slightly decreased, at earlier time points, but without reaching statistical significance. Remarkably, expression of both *Pck1* and *G6pc* genes was enhanced in profoundly hypoglycemic mutants at P1 compared with WT mice, strongly suggesting that their response to perinatal fasting is not impaired (Yubero *et al*, 2004).

Neonatal metabolic adaptations are orchestrated by changes in hormonal profiles, notably the decrease in the insulin/glucagon ratio that provokes glucose output by triggering hepatic glycogenolysis and transcriptional activation of key metabolic genes (Girard *et al*, 1992). As shown in Fig 3E, insulin levels at E19.5 + 4 dropped to the same range in both ΔMat and WT neonates relative to E19.5. Over the same time course, glucagon levels did not change significantly (Fig 3F), resulting in the decrease of insulin/glucagon ratios in both WT and ΔMat neonates. In addition, when P0 ΔMat neonates were arbitrarily split into two groups according to their glycemia, individuals with lower glucose concentration had decreased insulin contents (Fig 3E, right histogram). Glucagon levels were in the same range (Fig 3F, right histogram). Although we cannot formally rule out the possibility that the glucagon and/or insulin signaling cascades are impaired in ΔMat newborn's livers, these data argue for a normal pancreatic hormonal release, excluding hyperinsulinemia as a plausible cause for the neonatal hypoglycemia.

Genetic ablation of the miR-379/miR-410 cluster alters ketone levels in profoundly hypoglycemic mutants

The suckling period brings profound changes in nutrition since mother's milk consists of a high-fat diet. To face this sudden increase in the availability of fatty acids, neonates activate lipid oxidation pathways, mainly in the liver where fatty acids are also used as precursors for the synthesis of ketone bodies—acetoacetate, β-hydroxybutyrate and acetone—used as alternative fuel for maintaining adequate energy supplies for vital organs such as the brain (Girard *et al*, 1992). We next assessed ketone production (ketogenesis) by measuring β-hydroxybutyrate levels. As shown in Fig 4A, β-hydroxybutyrate levels in ΔMat neonates at P0 were in the normal range compared to WT, whereas, at P1, the most severely hypoglycemic mutants displayed lower levels. This decrease in β-hydroxybutyrate levels was observed without any apparent change in the availability of seric free fatty acids (Fig 4B) whereas triglyceride levels at P1 were significantly diminished (Fig 4C). Moreover, no significant changes in lipid contents were observed in mutant newborn livers at P1 (Fig 4D–G).

We next checked the expression of the carnitine palmitoyl transferase (*Cpt1a*) and 3-methylglutaryl-CoA synthase 2 (*Hmgcs2*) genes that control the entry of long-chain fatty acids into mitochondria and catalyze the first and rate-limiting step in ketogenesis, respectively. Expression of *Cpt1a* and *Hmgcs2* was diminished in ΔMat neonates at P1 regardless of their hypoglycemic status (Fig 4I), suggesting that ΔMat neonates do not properly activate ketogenesis pathways. Complete hepatic palmitate beta-oxidation activity measured in ΔMat pups at P0, as judged by the release of CO_2 (Fig 4J), was in the normal range as compared to WT. Of note, ΔMat mutants with severe hypoglycemia at P1 had lower milk content in their stomach (Fig 4H). Altogether, these results suggest that a reduction in milk suckling and in subsequent fatty acid supply, associated with defects in the expression of *Cpt1a* and *Hmgcs2,* likely underlie the low concentration of circulating ketone bodies. Alternatively, a decrease in ketone levels could also reflect an increase in their utilization by peripheral tissues, perhaps as a compensatory mechanism in the context of hypoglycemia.

Genetic ablation of the miR-379/miR-410 cluster affects the activation of neonatal hepatic gene expression

The hepatic expression profile of the miR-379/miR-410 cluster is relatively constant at the fetal–neonatal transition, yet it declines thereafter with very low, if any, expression from P28 (Supplementary Fig S4). To identify disrupted gene regulatory pathways that may contribute to deficiencies in maintaining neonatal energy homeostasis, we carried out mRNA gene expression profiling on WT and ΔMat livers dissected at E19.5, E19.5 + 4, and P0 (Supplementary Figs S5 and S6). The impact of ΔmiR on the transcriptome was relatively modest at E19.5 and E19.5 + 4, with only 13 and 139 mis-regulated genes, respectively, making it very unlikely that the miR-379/miR-410 cluster contributes significantly to the prenatal hepatic differentiation program. This is in stark contrast to P0, when important changes in gene expression were observed for as many as 1,836 mis-expressed transcripts: Of those, five genes, *Cyp2e1, Acnat2, Ces3b, Hsd17b6,* and as expected *Mirg*, were deregulated at all tested stages (Fig 5A, top). A list of the top 30

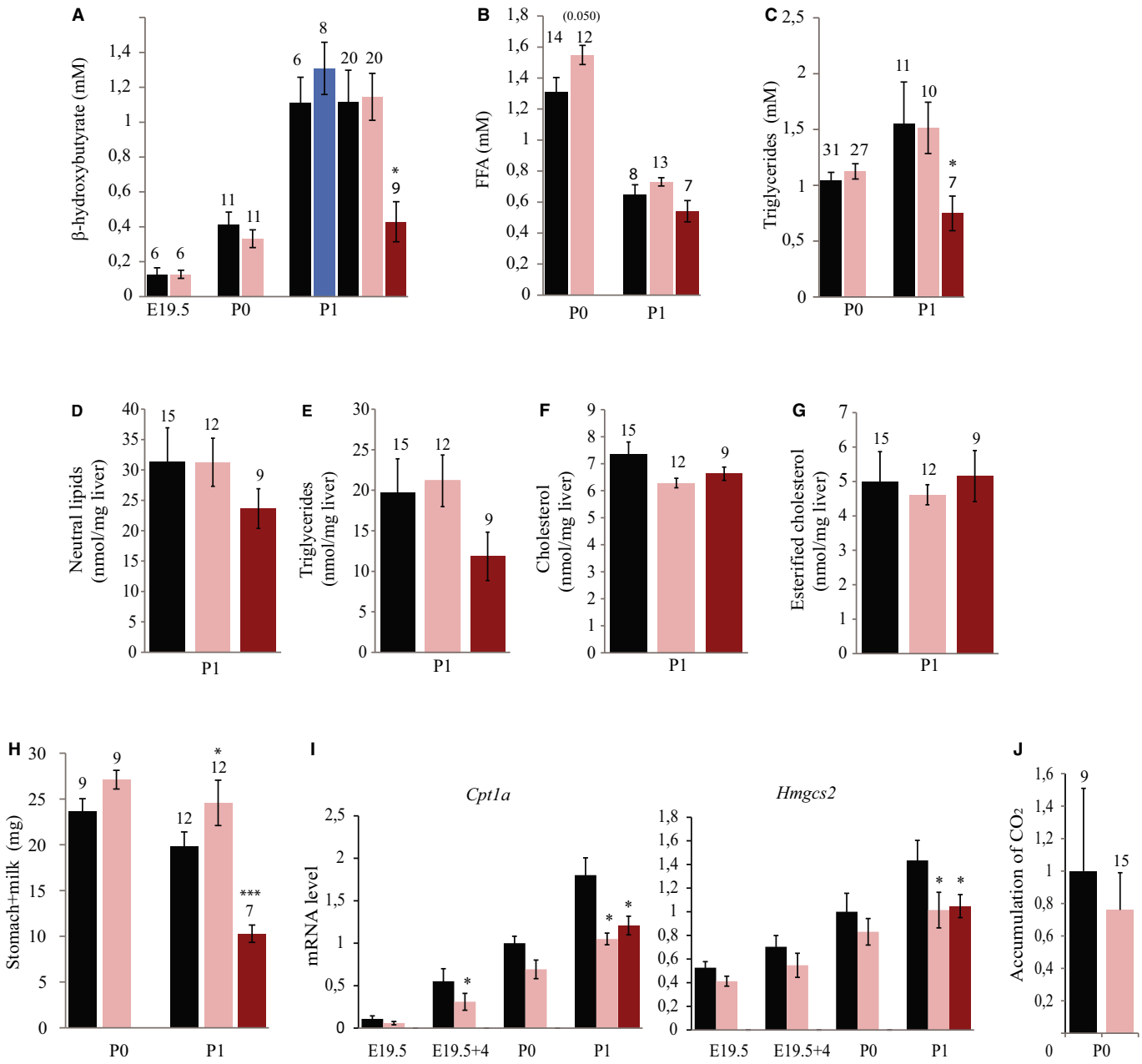

Figure 4. Maternal, but not paternal, deletion of the miR-379/miR-410 cluster impairs hepatic ketogenesis.

A–H Serum β-hydroxybutyrate (A), serum fatty acids (B), serum triglycerides (C), hepatic neutral lipids (D), hepatic triglycerides (E), hepatic cholesterol (F), hepatic esterified cholesterol (G), and stomach milk (H) levels were measured in WT (black), ΔMat (pink), severely hypoglycemic ΔMat (dark pink), or ΔPat (blue) individuals at E19.5 after cesarean delivery or P0 and P1 after vaginal delivery.

I Temporal expression of the ketogenic *Cpt1a* and *Hmgcs2* genes was assayed in the liver (relative to *Gapdh*) by RT–qPCR (6 individuals per genotype).

J The complete hepatic beta-oxidation of ^{14}C-labelled palmitate at P0 was determined by the release of ^{14}C-labelled CO_2. Beta-oxidation activities for WT were set to 1.

Data information: Data are expressed as mean ± s.e.m.

up- and down-regulated protein-coding genes at P0 is given in Fig 5A (bottom). Note that ΔmiR does not impact on the perinatal expression of the surrounding imprinted genes (Supplementary Fig S4). We conclude from these results that major gene deregulation occurs in ΔMat livers at the developmentally regulated birth transition.

In agreement with these microarray data, mRNA expression levels of some selected genes were significantly reduced (Fig 5B, left) or increased (Fig 5B, right) at P0 in neonatal ΔMat liver compared to WT littermates. Their expression in ΔPat neonatal livers remained mostly unaffected. Results of our analysis for the enrichment of Gene Ontology (GO) Biological Processes and Kyoto

Encyclopedia of Genes and Genomes (KEGG) pathways showed that down-regulated genes are enriched for genes involved in metabolic processes, notably lipid metabolism (Supplementary Fig S7; see GO terms 'cellular ketone metabolic process', 'lipid metabolism', 'fatty acid metabolic process', and KEGG pathways for 'fatty acid metabolism', 'peroxisome', 'PPAR signaling', 'bile secretion', 'metabolism of xenobiotics by cytochrome P450'). Enrichment of functional categories among the up-regulated genes was less apparent. Among down-regulated genes, Fibroblast growth factor 21 (*Fgf21*) has recently emerged as a potent endocrine regulator of lipid metabolism, notably in response to a ketogenic diet (Potthoff *et al*, 2012). It also contributes to neonatal metabolic adaptation by controlling thermogenic activation (Hondares *et al*, 2010). *Nr0b2*/SHP is an orphan nuclear receptor that lacks a DNA-binding domain and plays pleiotropic transcriptional regulatory roles in numerous biological functions, notably in cholesterol, bile acid, and fatty acid metabolism (Zhang *et al*, 2011). Cyp2e1, a member of the cytochrome P450 superfamily, catalyzes many reactions involved in drug metabolism, including that of ethanol, as well as in the synthesis of steroids, cholesterol, and other lipids (Cederbaum, 2010). Of note, Cyp2e1 is also involved in ketone metabolism and participates in an alternative gluconeogenesis pathway (Gonzalez, 2007).

Importantly, we noticed that ~75% of the most significant misexpressed genes at P0 (fold-change > 1.7; 410/547) correspond to down-regulated genes in ΔMat neonates. This also holds true at E19.5 + 4, when this proportion reaches 90% (56/62). Moreover, hierarchical clustering (Fig 5C) identifies two major clusters that correspond to genes with increased (group 1) or decreased (group 2) expression in mutant vs WT livers at P0. Within each cluster, subclusters can be defined according to different temporal patterns of changes in gene expression between E19.5 and P0: Sub-cluster A corresponds to genes that exhibit major changes in expression in ΔMat but not in WT mice between E19.5 and P0 (up-regulation for cluster 1A and down-regulation for cluster 2A). Conversely, subcluster B corresponds to genes with major changes in expression between E19.5 and P0 in WT (up-regulation for cluster 1B and down-regulation for cluster 2B), but not in ΔMat livers. Defects in the temporal expression of some down-regulated genes belonging to clusters 2A or 2B were further assayed by RT–qPCR. As reported in Figure 5D, expression of *Fgf21, Cyp2e1, Nr0b2, Dio1, Bdh1, Igf1,* and *Slc17a2* was up-regulated at P0 in WT livers, whereas the timing and/or magnitude of their up-regulation were significantly affected in ΔMat livers.

Those data are consistent with a model according to which ΔmiR causes a delayed transition in the activation of hepatic gene expression. Indeed, when mRNA profiling experiments were performed at P1 by selecting ΔMat pups with mild and severe hypoglycemia, the overall impact of ΔmiR was less pronounced than that reported at P0 (Supplementary Figs S8 and S9). This reinforces the important notion that the major impact of ΔmiR in the liver occurs precisely in the narrow temporal window coinciding with birth transition. In light of the partial penetrance of the metabolic phenotype, it is of interest that hepatic transcriptome defects of ΔMat mutants with mild hypoglycemia were largely resolved at P1 while profoundly hypoglycemic mutants exhibited sustained alterations in gene expression. Taken together, these unbiased genome-wide studies uncover a liver-specific, miRNA-controlled gene expression program whose sustained perturbation is very likely to underlie the metabolic deficiencies and lethality observed in a subset of ΔMat neonates. Accordingly, the miR-379/miR-410 cluster emerges as a potent candidate regulator of the neonatal hepatic gene expression program (Fig 6).

Discussion

Results of our study demonstrate, at the whole-organism level, that the maternally expressed miR-379/miR-410 cluster plays essential roles in neonatal survival. They provide, to the best of our knowledge, the first demonstration that miRNAs can be implicated in the balance of adaptive metabolic changes that occur at the transition from prenatal to postnatal life: Newly born pups have to combat neonatal hypoglycemia and must rapidly switch from the use of glucose to that of lipids provided by mother's milk (Girard *et al*, 1992). This illustrates another outstanding example of miRNAs as part of regulatory systems that shape important developmental transitions, as already shown in *C. elegans* (Ambros, 2011), zebrafish (Giraldez, 2010), and plants (Poethig, 2009). Our work also lends further experimental support to the emerging notion that defects in mammalian miRNA-mediated regulation yield phenotypic consequences mostly under conditions of physiological, metabolic, and/or environmental changes (Leung & Sharp, 2010; Mendell & Olson, 2012).

Genetic ablation of the miR-379/miR-410 cluster does not lead to overt developmental abnormalities, ruling out any major contribution to embryonic lethality or even to reprogramming defects of induced pluripotent stem cells, as previously observed in several mouse models where all maternally expressed non-coding RNA genes at the *Dlk1-Dio3* region were silenced (Lin *et al*, 2003; da Rocha *et al*, 2008; Liu *et al*, 2010; Stadtfeld *et al*, 2010). Importantly, nearly half of ΔMat neonates do not overcome the critical immediate perinatal period because of severe metabolic abnormalities.

Figure 5. Loss of the miR-379/miR-410 cluster is associated with major changes in the neonatal hepatic gene expression program.

A Top: Venn diagrams showing the number of up- and down-regulated genes revealed by Agilent microarrays at E19.5, E19.5 + 4, and P0 in ΔMat and WT livers (BH-adjusted *P*-value < 0.05). Bottom: Top 30 of up- and down-regulated genes. ncRNA genes and other poorly characterized transcripts, except the microRNA host gene (*Mirg*), were omitted from this microarray list.

B Expression levels of selected misregulated genes validated by RT–qPCR. Blue and pink bars represent expression levels in ΔPat and ΔMat individuals, respectively. WT expression levels were arbitrarily set to 1.

C Heatmap and hierarchical clustering of genes regulated in ΔMat vs. WT newborn livers at E19.5 or P0 (2,147 unique probes with BH-adjusted *P*-value < 0.05). Red: up-regulated; green: down-regulated; black: no change.

D Perinatal expression of some genes was assayed by RT–qPCR analysis. Black and pink bars indicate expression levels in ΔPat and ΔMat individuals, respectively. Dark pink represents the most hypoglycemic mutant neonates at P1. WT expression levels at P0 were arbitrarily set to 1. Note that the dramatic decrease in *Fgf21* mRNA levels in P1 hypoglycemic neonates may reflect the fact that fasting neonates display lower levels of *Fgf21* expression (Hondares *et al*, 2010).

Data information: Data in (B–D) are expressed as mean ± s.e.m. (n = 4–6 individuals per genotype).

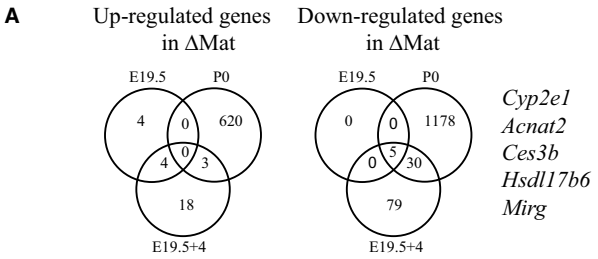

Top30 up- and down-regulated genes in neonatal (P0) liver

Up/logFC				Down/logFC			
Fibin	2.75	Doc2b	1.52	Cyp2e1	-3.27	Ostb	-1.81
Serpina3i	2.74	Zbtb16	1.51	Prok1	-3.18	Cyp3a59	-1.81
Fam134b	2.21	Ddit4	1.48	**Mirg**	**-2.71**	Acot3	-1.80
Cidea	2.17	Fam107a	1.48	Fgf21	-2.31	Hsd3b4	-1.79
Lpin1	2.04	Adra2a	1.47	Akr1c6	-2.27	Fgf1	-1.77
Hamp	1.99	Tmc7	1.47	Nr0b2	-2.18	Inmt	-1.74
Slco4c1	1.97	Ctsj	1.45	Cyp2d37-ps	-2.16	Otc	-1.73
Setdb2	1.96	Itgae	1.45	Inhbe	-2.09	Dio1	-1.73
Sds	1.88	trp53inp1	1.44	Acnat2	-2.02	Ces3b	-1.70
Esrrg	1.80	Ppp1r3g	1.42	Cyp1a2	-2.01	Mettl7b	-1.68
Map3k6	1.79	Esm1	1.41	Akr1c20	-2.00	Acnat2	-1.66
Chac1	1.77	Isg15	1.36	Slc22a1	-1.95	Slco1b2	-1.64
Gpr88	1.71	Upp2	1.35	Sult1c2	-1.87	Gpd1	- 1.64
O3far1	1.61	Il1r2	1.33	Cyp2f2	-1.86	Crot	-1.64
Got1	1.54	Sgk1	1.31	Ugtb35	-1.81	Apol7a	-1.63

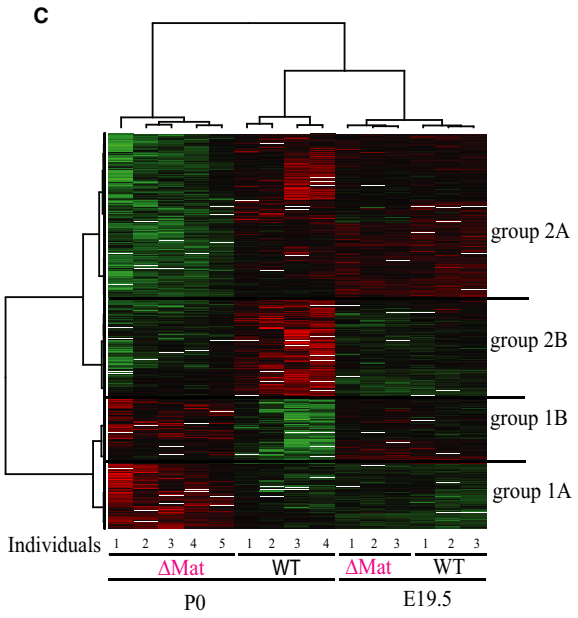

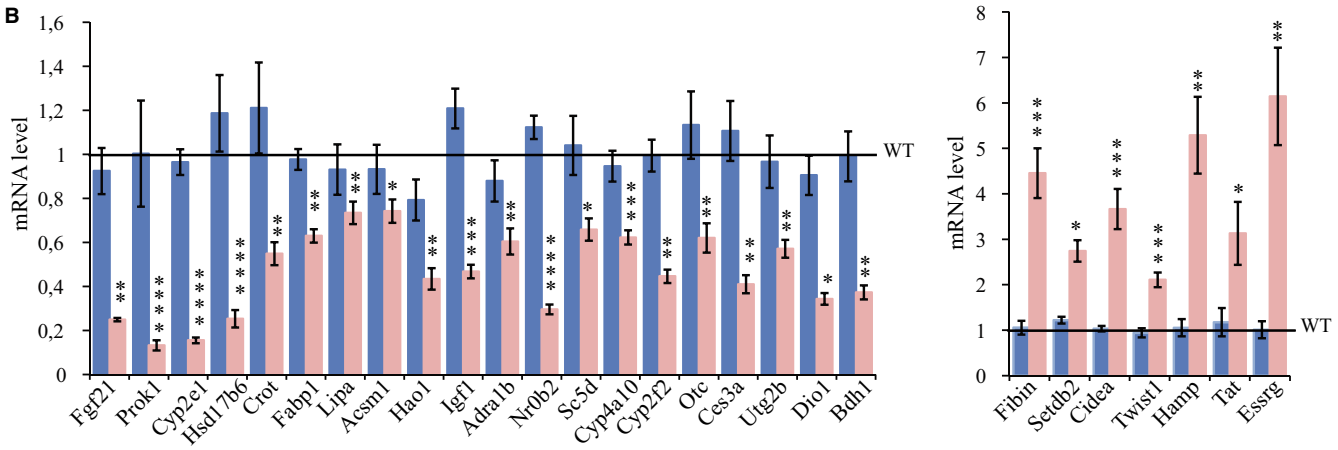

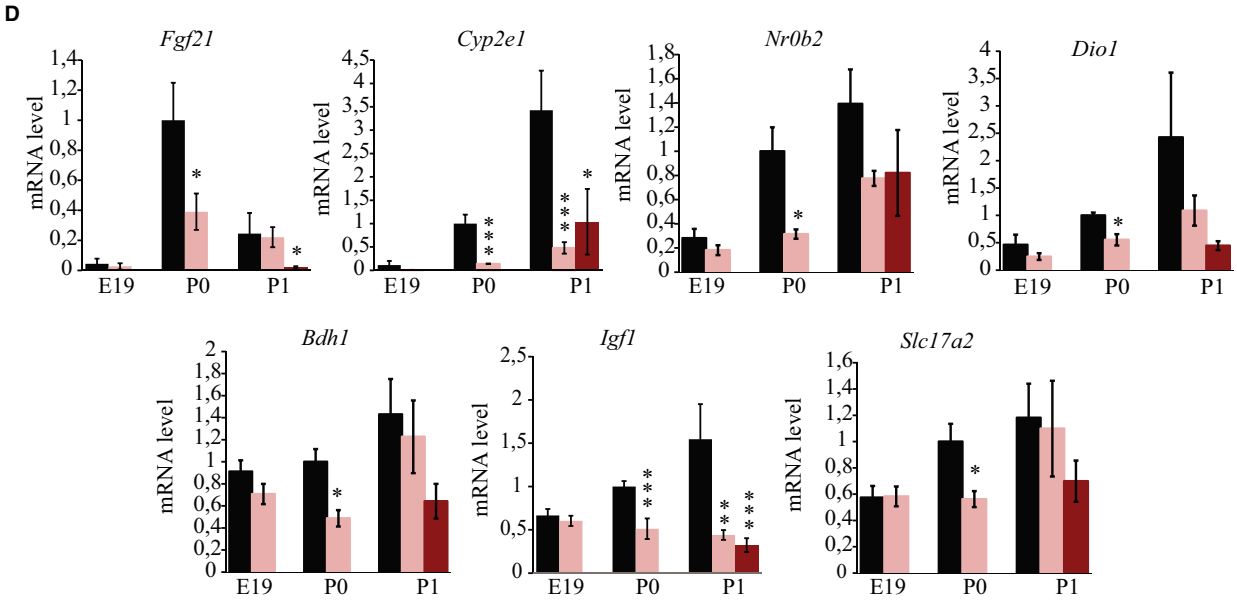

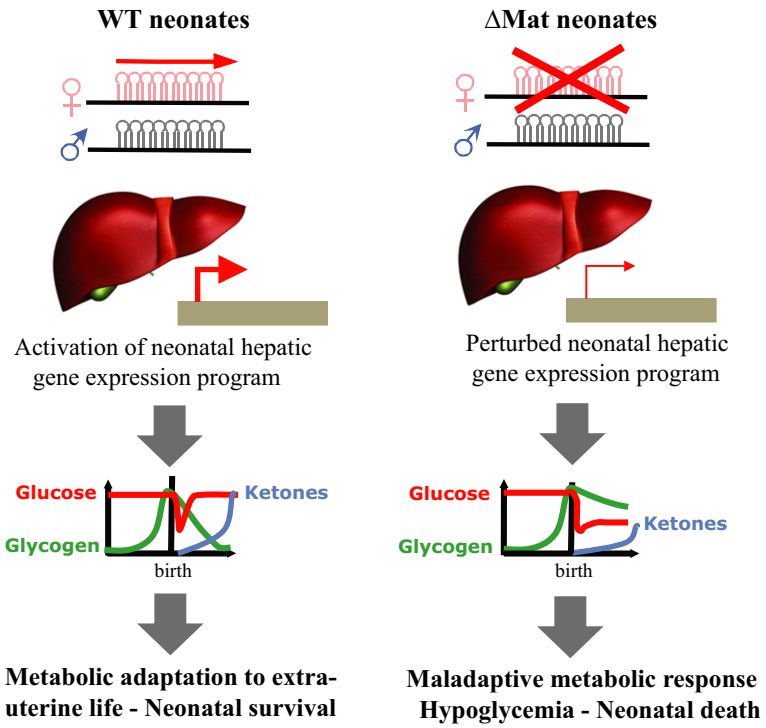

Figure 6. The miR-379/miR-410 cluster controls metabolic adaptation at the transition from fetal to postnatal life.
Our model implies that maternally inherited deletion of the miR-379/miR-410 cluster interferes with the activation (or maintenance) of the neonatal hepatic gene program at the transition from fetal to postnatal life. This results in interlaced defects in the newborn (P0–P1) liver that include inefficient mobilization of hepatic glycogen stores, defective gluconeogenesis pathways and the inability to compensate with elevated levels of ketone bodies. Such a pleiotropic maladaptive metabolic response—in the absence of any apparent defects in pancreatic hormonal release—leads to severe neonatal hypoglycemia which most likely represents the main, if not the sole, cause of subsequent death.

Appropriate dosage of the *Dlk1* and *Dio3* genes is also crucial for metabolic and environmental adaptation when mice reach independent feeding and temperature control (Charalambous *et al*, 2012). Strikingly, ΔMat pups also display transient postnatal growth retardation. This coincides with the weaning transition, possibly reflecting a role for the miR-379/miR-410 cluster in related physiological pathways that implicate its neighboring *Dlk1* and *Dio3* paternally expressed protein-coding genes. Taken together, these findings support the view that imprinted genes in general, and the *Dlk1-Dio3* domain in particular, exert important postnatal metabolic functions, in addition to their known roles in mammalian development (Constancia *et al*, 2004; Charalambous *et al*, 2007, 2014; Frontera *et al*, 2008).

The newborn's liver ensures a crucial metabolic adaptation in the immediate perinatal period in relation to nutritional, hormonal, and/or environmental changes, but the transcriptional regulatory circuitry that triggers glucose output and activates lipid oxidation pathways remains poorly understood. Our observations that ΔMat neonates fail to engage this switch in timely fashion demonstrate that some—or all—of the deleted miRNA genes help regulate the required underlying transcriptional response. This is exemplified by delayed (or decreased) expression of hundreds of genes whose expression must be turned on (or maintained) during the immediate perinatal period, for example *Cpt1a* (Thumelin *et al*, 1994), *Cyp2e1* (Hart *et al*, 2009), *Pck1* (Wang *et al*, 1995), *Fgf21* (Hondares *et al*, 2010). Although we do not fully understand how the miR-379/miR-410 cluster may confer, directly or indirectly, robustness to neonatal hepatic transcriptional regulatory circuits, our findings are consistent with a model whereby loss of miRNA expression is mostly, if not exclusively, detrimental during a very narrow temporal window just before—or coinciding with—birth, when neonates mount, for the first time, adaptive metabolic responses.

Although not unusual in genetically modified animals, including in miRNA-deficient mice (Medeiros *et al*, 2011), the reasons for the incomplete penetrance of the neonatal lethality phenotype remain difficult to formulate. Lethality in a given litter was observed regardless the number of ΔMat pups, the ratio of ΔMat vs WT, the parental origin of the deletion in the dams, and the length of gestation or even number of pregnancies the dams had experienced. Any genetic background effects appear unlikely since neonatal death is observed after more than 10 backcrosses on C57BL/6J background. That ΔMat individuals with mild hypoglycemia re-expressed the miR-379/miR-410 cluster from the normally silent paternal allele can also be ruled out (Supplementary Fig S4). Fluctuations in gene expression can give rise to phenotypic variations if expression levels that underlie an outcome are subjected to a threshold (Raj *et al*, 2010). Loss of the miR-379/miR-410 cluster most likely leads to variability in the timing of expression of some metabolic genes and, beyond a certain threshold, to mis-expression of some of them, particularly those encoding rate-limiting enzymes. This may cause complex and interconnected hepatic dysfunctions that affect both glucose and lipid metabolism. We reason that ΔmiR first disrupts glucose homeostasis in most, if not all, ΔMat mutants. These deficiencies may in turn decrease the ability of some lethargic pups to

compete efficiently for suckling (hence low milk intake and low ketone levels in mutants with severe hypoglycemia at P1). A 'butterfly effect' (Dorn, 2013) whose phenotypic consequences are mostly, if not exclusively, observed at birth because it represents the first drastic survival-challenging event might account for some aspects of the incomplete penetrance we observe. We are speculating that the ability 'to suckle in time' may also allow some ΔMat neonates to recover and also perhaps to resolve their alterations in hepatic transcriptome. Given the constitutive deletion of the miRNA cluster, we cannot exclude the possibility that lack of miRNA expression in other tissues not investigated in this study, for example, the newborn's brain, also impacts on this complex neonatal metabolic phenotype.

The question of the identity of the repertoire of mRNAs that are presumably silenced by the miR-379/miR-410 cluster remains open. The large number of deleted miRNA genes renders illusory —if not naïve—a concentration of too much effort on *in silico* predictions: Assuming that all miRNAs are equally functional, bioinformatics identify over 10,000 mRNA targets. As a case in point, we could not find any statistical enrichment of binding sites for the deleted miRNAs within the 3′-UTR of up-regulated transcripts in neonatal liver, as would have been expected if miRNAs trigger significant RNA decay of their targets (Baek *et al*, 2008). Moreover, because the miR-379/miR-410 cluster is only found in eutherian species, this considerably limits further analysis that would take into account the phylogenetic conservation of miRNA:: mRNA base-pairings between evolutionarily distant species. Finally, we cannot rule out the possibility that miRNAs act through pure translational repression mechanisms or regulate their targets by non-canonical interactions (Helwak *et al*, 2013), hindering further *in silico* searches. More sensitive and unbiased genome-wide approaches, including the study of temporally induced, tissue-specific deletions, should help identify gene regulatory networks controlled by the miR-379/miR-410 cluster in the most biologically relevant tissues.

Pathways deregulated in ΔMat neonates mostly relate, but are not restricted, to aspects of lipid metabolism that are crucially engaged when a suckling-based, lipid-rich diet is initiated. In marsupials, milk composition changes gradually during the course of lactation (Brennan *et al*, 2007). This is in striking opposition to eutherians, which have to adapt to an abrupt transition in energy substrates. From an evolutionary perspective, we speculate that, once acquired at the *Dlk1-Dio3* chromosomal domain and amplified at the root of the eutherian lineage (Edwards *et al*, 2008), the miR-379/miR-410 cluster may have functionally converged toward postnatal regulatory roles at the transition from fetal to postnatal life. This might have possibly extended to the weaning transition to independent life, which also entails profound nutritional changes. Acquisition of the miR-379/miR410 cluster in eutherian species may have increased neonate fitness by improving their metabolic adaptability upon profound changes in nutrition. If so, this may have contributed to placental mammal evolution.

How the ΔMat phenotypes relate to the complex epigenetic pathways that ultimately drive selection for the maternal expression of the miR-379/miR-410 cluster remains unknown. Although still a matter of active and lively debate, several theories attempt to explain the evolutionarily meaning of the emergence of paternally and maternally expressed genes in mammals (Kaneko-Ishino *et al*, 2003; Wilkins & Haig, 2003; Wolf & Hager, 2006), yet none of them account for all consequences of imprinting of genes. One of these explanations, the broadly discussed 'conflict theory', states that paternally expressed genes favor acquisition of maternal resources. In contrast, maternally expressed genes would tend to counteract this effect by limiting the drain of resources in the mother (Moore & Haig, 1991). While the silencing of the paternally expressed *Rtl1* gene in the placenta by the maternally expressed miR-127/miR-136 cluster, also positioned at the *Dlk1-Dio3* domain, satisfies to some extent the predictions of the conflict theory (Seitz *et al*, 2003; Davis *et al*, 2005; Lewis & Redrup, 2005; Sekita *et al*, 2008), the lack of major developmental defects and the postnatal phenotypes associated with full deletion of the miR-379/miR-410 cluster do not easily fit with this simple view. A better understanding of why imprinting has evolved is still lacking to fully appreciate the significance of the mono-allelic expression of the miR-379/miR-410 cluster. It should also be noted that maternal expression of the miR-379/miR-410 cluster could simply be an evolutionary remnant whose *raison d'être* would simply result from 'bystander effects' due to long-range epigenetic regulations that orchestrate imprinted expression at the *Dlk1-Dio3* chromosomal region (Labialle & Cavaille, 2011).

We have shown that the very first hours of extra-uterine life, which are associated with unique metabolic adjustments, require one or several—if not all—miRNAs encoded within the imprinted miR-379/miR-410 cluster. Although we do not know whether additional defects occur elsewhere (including at earlier developmental stages) and are then transduced to the changes we observe in the transcriptional circuitry of the liver, it is clear that a maternally inherited deficiency of the miR-379/miR-410 cluster is sufficient to compromise implementation of the complex hepatic transcriptional program that normally occurs at birth. Targeted deletions of one (or a few) evolutionarily conserved miRNA gene(s) in the mouse have revealed that only very few null mutants display full (or partially penetrant) lethality phenotypes (Park *et al*, 2010, 2012). Our findings that the eutherian-specific miR-379/miR-410 cluster plays essential roles in neonatal survival and metabolic control at birth therefore provide important insights into the biological importance of recently evolved miRNA genes. In this context, it will be of interest to study other lineage-specific miRNA loci—particularly the two imprinted C19MC and *Sfmbt2* clusters that are found only in primates and rodents, respectively (Noguer-Dance *et al*, 2010; Wang *et al*, 2011).

Materials and Methods

Mice housing, breeding, embryo harvest

All animal procedures were approved by the University of Toulouse and CNRS Institutional Animal Care Committee (01503.01). The animal housing facility met CNRS standards. Mice were housed in standard plastic cages with access to food (rodent chow diet) and water *ad libitum* in a temperature-controlled room, with a 12-h light–dark cycle. Breeding was performed overnight. Female breeders positive for copulation plugs in the morning were considered embryonic day 0.5 (E0.5). Neonates were examined at the premorbid stage (10–15 h post-delivery, denoted as P0) and

within the window of lethality (30–35 h post-delivery, denoted as P1). For cesarean delivery, pups were immediately expelled and put in a warm and moist box placed in a 37°C water bath. Pups' mouths and nostrils were gently cleaned with cotton swabs, which were also used to stimulate breathing and motion by gentle massage. Pups were continuously monitored during the course of the experiment. All experiments were performed starting from the sixth generation of backcrossing in the C57BL/6J genetic background.

Targeted disruption of the miR-379/miR-410 cluster

A mouse model carrying a large ~59-kb-long deletion overlapping the entire miR-379/miR-410 cluster (ΔmiR) was generated by Cre/loxP-mediated site-specific deletion at the MCI/ICS (Mouse Clinical Institute, Illkirch, France). Briefly, two targeting vectors harboring neomycin- and hygromycin-resistance expression cassettes were introduced upstream and downstream, respectively, of the microRNA cluster. This was achieved through two independent homologous recombination events in 129Sv-derived embryonic stem (ES) cells. A positive ES cell with correct targeting on the same allele and displaying normal karyotype was injected into C57BL/6J host blastocysts, and chimeras were produced. Chimeric males that passed the targeted allele to their offspring were mated with Cre-deleter females (CMV-Cre), and the entire cluster was faithfully excised *in vivo*. PCR genotyping was performed on genomic DNA prepared from tails of embryonic, neonatal, or weaned mice, using the Wizard SV Genomic DNA Purification System (Promega) kit. Wild-type and targeted alleles were amplified using P1/P2 and P1/P3 oligonucleotide pairs, respectively (Fig 1C). Primer sequences are listed in Supplementary Fig S10.

Blood and metabolic parameter analysis

Glucose levels were measured using a hand-held blood glucose meter (Accu-check Performa, Roche Diagnostics). Samples below the detection limit (10 mg/dl) were arbitrarily set to 9 mg/dl. Hepatic glycogen was assayed by a direct enzymatic procedure. Fresh or frozen livers were homogenized in 1N NaOH at 55°C and then neutralized with 1 volume of 1N HCl. Samples were treated with 50 U/ml amyloglucosidase (Sigma) in 0.2 M sodium acetate at pH 4.8 for 1 h at 55°C to convert glycogen to glucose monomers. Glucose was quantified using the Glucose (GO) Assay Kit (Sigma). Circulating levels of ketone bodies were quantified using the β-hydroxybutyrate (Ketone Body) Assay kit (Cayman Chemical Company). Quantification of insulin and glucagon was performed using the MILLIPLEX MAP Mouse Metabolic Disease Panel (Merck Millipore) and analyzed with the Luminex 100 IS apparatus at the IBISA-labeled Transgenesis, Zootechny and Functional Exploration Core Facility of Toulouse (Anexplo/GenoToul). Serum-free fatty acid and triglyceride analyses were also performed there with the ABX PENTRA400 analyzer. Lipidomic analysis was performed at the Toulouse INSERM Metatoul-Lipidomique Core Facility. Lipids corresponding to 1 mg of tissue were extracted and analyzed by gas-liquid chromatography on a FOCUS Thermo Electron system using Zebron-1 Phenomenex-fused silica capillary columns (Barrans *et al*, 1994). For measurement of beta-oxidation, newborn's livers were minced and hepatocytes were isolated after collagenase digestion. Isolated hepatocytes were then incubated with 0.5 μCi/ml of ^{14}C-labelled palmitate, and complete fatty acid oxidation was determined by the release of ^{14}C-labelled CO_2 (Attane *et al*, 2012).

RNA extraction, quantitative real-time PCR, Northern blot analysis

Total RNA was extracted using TRI reagent (Euromedex) according to the manufacturer's instructions followed by RNase-free RQ1 DNAse (Promega) and proteinase K (Sigma) treatments or purification with RNeasy column (Qiagen). mRNA expression was determined using the Go Script™ Reverse Transcriptase (Promega) kit, and amplifications were performed using the IQ™ Custom SYBR Green Supermix (Bio-Rad) qPCR kit. miRNA expression was measured using the miScript Reverse Transcription kit and the miScript SYBR Green PCR kit (Qiagen), using specific primers (Qiagen) and *U6* RNA as an endogenous control. cDNAs were amplified on an Analytik Jena Flexcycler. Primer sequences are listed in Supplementary Fig S10. Total RNA (10 μg) was fractionated by electrophoresis on a 15% acrylamide/7M urea denaturating gel. Electrotransfer was performed onto nylon membranes (BrightStar Plus membrane, Ambion), followed by UV-light irradiation. Northern blot hybridization was carried out with 5′-^{32}P-labeled DNA oligonucleotide probes, with an overnight incubation at 50°C in 5× SSPE, 1% SDS, 5× Denhardt's, and 150 μg/ml yeast tRNA. Membranes were washed twice in 0.1% SSPE and 0.1% SDS at room temperature before autoradiography.

Transcriptome analysis

mRNA gene expression profiles were performed at the GeT-Trix facility (Toulouse) using Agilent Whole Mouse Genome microarrays (8 × 60 k) according to the manufacturer's instructions. Microarray data and all experimental details are available in the Gene Expression Omnibus (GEO) database (accession numbers GSE47159 and GSE57112).

Statistical methods

Results are expressed as mean ± s.e.m. Comparison of two groups was analyzed by a two-tailed Student's unpaired *t*-test. Deviation from Mendelian frequencies was analyzed by a χ^2 test. Statistically significant differences between groups are indicated as $^*P < 0.05$, $^{**}P < 0.01$, $^{***}P < 0.001$ and $^{****}P < 0.0001$.

Supplementary information for this article is available online: http://emboj.embopress.org

Acknowledgements

This work is dedicated to the memory of our colleague and friend E. Käs. We thank Y. Henry for careful reading of the manuscript and A. Ferguson-Smith, D. Langin, P. Ferré, L. Casteilla, J. Girard, A. Lorsignol, and F. Villarroyal for informal discussions throughout this work. We are indebted to Jacques Auriol, Séverine Ethuin and Frederic Luce (from the Zootechnie ABC) for their technical assistance during the week-end. We are also grateful to Y. Lippi, G. Canal, and H. Seitz for help in microarray analyses, R software and the search of miRNA targets, respectively. This work was supported by grants from European Union (CallimiR), EMBO (EMBO Young Investigator Programme), and ANR (ImpmiR).

Author contributions

SL and VM performed and analyzed most of the experiments. M-LB-C performed some RT–qPCR and Northern blot experiments. MH-O initiated the phenotypic characterization of miR mice. J-PP and PV contributed to the design and analysis of fatty acid beta-oxidation in the newborn's liver. PM supervised transcriptomic experiments and interpreted the data. JC and SL conceived the project and wrote the manuscript with some inputs from other authors.

Conflict of interest

The authors declare that they have no conflict of interest.

References

Ambros V (2011) MicroRNAs and developmental timing. *Curr Opin Genet Dev* 21: 511 – 517

Attane C, Foussal C, Le Gonidec S, Benani A, Daviaud D, Wanecq E, Guzman-Ruiz R, Dray C, Bezaire V, Rancoule C, Kuba K, Ruiz-Gayo M, Levade T, Penninger J, Burcelin R, Penicaud L, Valet P, Castan-Laurell I (2012) Apelin treatment increases complete Fatty Acid oxidation, mitochondrial oxidative capacity, and biogenesis in muscle of insulin-resistant mice. *Diabetes* 61: 310 – 320

Baek D, Villen J, Shin C, Camargo FD, Gygi SP, Bartel DP (2008) The impact of microRNAs on protein output. *Nature* 455: 64 – 71

Barlow DP, Bartolomei MS (2014) Genomic imprinting in mammals. *Cold Spring Harb Perspect Biol* 6: pii: a018382 .

Barrans A, Collet X, Barbaras R, Jaspard B, Manent J, Vieu C, Chap H, Perret B (1994) Hepatic lipase induces the formation of pre-beta 1 high density lipoprotein (HDL) from triacylglycerol-rich HDL2. A study comparing liver perfusion to in vitro incubation with lipases. *J Biol Chem* 269: 11572 – 11577

Benetatos L, Voulgaris E, Vartholomatos G (2012) DLK1-MEG3 imprinted domain microRNAs in cancer biology. *Crit Rev Eukaryot Gene Expr* 22: 1 – 15

Bicker S, Khudayberdiev S, Weiss K, Zocher K, Baumeister S, Schratt G (2013) The DEAH-box helicase DHX36 mediates dendritic localization of the neuronal precursor-microRNA-134. *Genes Dev* 27: 991 – 996

Brennan AJ, Sharp JA, Digby MR, Nicholas KR (2007) The tammar wallaby: a model to examine endocrine and local control of lactation. *IUBMB Life* 59: 146 – 150

Bushati N, Cohen SM (2007) microRNA functions. *Annu Rev Cell Dev Biol* 23: 175 – 205

Cederbaum AI (2010) Role of CYP2E1 in ethanol-induced oxidant stress, fatty liver and hepatotoxicity. *Dig Dis* 28: 802 – 811

Charalambous M, da Rocha ST, Ferguson-Smith AC (2007) Genomic imprinting, growth control and the allocation of nutritional resources: consequences for postnatal life. *Curr Opin Endocrinol Diabetes Obes* 14: 3 – 12

Charalambous M, Ferron SR, da Rocha ST, Murray AJ, Rowland T, Ito M, Schuster-Gossler K, Hernandez A, Ferguson-Smith AC (2012) Imprinted gene dosage is critical for the transition to independent life. *Cell Metab* 15: 209 – 221

Charalambous M, da Rocha ST, Hernandez A, Ferguson-Smith AC (2014) Perturbations to the IGF1 growth pathway and adult energy homeostasis following disruption of mouse chromosome 12 imprinting. *Acta Physiol (Oxf)* 210: 174 – 187

Chiang HR, Schoenfeld LW, Ruby JG, Auyeung VC, Spies N, Baek D, Johnston WK, Russ C, Luo S, Babiarz JE, Blelloch R, Schroth GP, Nusbaum C, Bartel DP (2010) Mammalian microRNAs: experimental evaluation of novel and previously annotated genes. *Genes & Development* 24: 992 – 1009

Christensen M, Larsen LA, Kauppinen S, Schratt G (2010) Recombinant adeno-associated virus-mediated microRNA delivery into the postnatal mouse brain reveals a role for miR-134 in dendritogenesis in vivo. *Front Neural Circuits* 3: 16

Constancia M, Kelsey G, Reik W (2004) Resourceful imprinting. *Nature* 432: 53 – 57

Davis E, Caiment F, Tordoir X, Cavaille J, Ferguson-Smith A, Cockett N, Georges M, Charlier C (2005) RNAi-mediated allelic trans-interaction at the imprinted Rtl1/Peg11 locus. *Curr Biol* 15: 743 – 749

Dorn GW 2nd (2013) MicroRNAs and the butterfly effect. *Cell Cycle* 12: 707 – 708

Edwards CA, Mungall AJ, Matthews L, Ryder E, Gray DJ, Pask AJ, Shaw G, Graves JA, Rogers J, Dunham I, Renfree MB, Ferguson-Smith AC (2008) The evolution of the DLK1-DIO3 imprinted domain in mammals. *PLoS Biol* 6: e135

Fabian MR, Sonenberg N (2012) The mechanics of miRNA-mediated gene silencing: a look under the hood of miRISC. *Nat Struct Mol Biol* 19: 586 – 593

Fiore R, Khudayberdiev S, Christensen M, Siegel G, Flavell SW, Kim TK, Greenberg ME, Schratt G (2009) Mef2-mediated transcription of the miR379-410 cluster regulates activity-dependent dendritogenesis by fine-tuning Pumilio2 protein levels. *EMBO J* 28: 697 – 710

Frontera M, Dickins B, Plagge A, Kelsey G (2008) Imprinted genes, postnatal adaptations and enduring effects on energy homeostasis. *Adv Exp Med Biol* 626: 41 – 61

Gao J, Wang WY, Mao YW, Graff J, Guan JS, Pan L, Mak G, Kim D, Su SC, Tsai LH (2010) A novel pathway regulates memory and plasticity via SIRT1 and miR-134. *Nature* 466: 1105 – 1109

Giraldez AJ (2010) microRNAs, the cell's Nepenthe: clearing the past during the maternal-to-zygotic transition and cellular reprogramming. *Curr Opin Genet Dev* 20: 369 – 375

Girard J, Ferre P, Pegorier JP, Duee PH (1992) Adaptations of glucose and fatty acid metabolism during perinatal period and suckling-weaning transition. *Physiol Rev* 72: 507 – 562

Girardot M, Cavaille J, Feil R (2012) Small regulatory RNAs controlled by genomic imprinting and their contribution to human disease. *Epigenetics* 7: 1341 – 1348.

Gonzalez FJ (2007) The 2006 Bernard B. Brodie Award Lecture. Cyp2e1. *Drug Metab Dispos* 35: 1 – 8

Hart SN, Cui Y, Klaassen CD, Zhong XB (2009) Three patterns of cytochrome P450 gene expression during liver maturation in mice. *Drug Metab Dispos* 37: 116 – 121

Helwak A, Kudla G, Dudnakova T, Tollervey D (2013) Mapping the human miRNA interactome by CLASH reveals frequent noncanonical binding. *Cell* 153: 654 – 665

Hondares E, Rosell M, Gonzalez FJ, Giralt M, Iglesias R, Villarroya F (2010) Hepatic FGF21 expression is induced at birth via PPARalpha in response to milk intake and contributes to thermogenic activation of neonatal brown fat. *Cell Metab* 11: 206 – 212

Jimenez-Mateos EM, Engel T, Merino-Serrais P, McKiernan RC, Tanaka K, Mouri G, Sano T, O'Tuathaigh C, Waddington JL, Prenter S, Delanty N, Farrell MA, O'Brien DF, Conroy RM, Stallings RL, DeFelipe J, Henshall DC (2012) Silencing microRNA-134 produces neuroprotective and prolonged seizure-suppressive effects. *Nat Med* 18: 1087 – 1094

Kagami M, Sekita Y, Nishimura G, Irie M, Kato F, Okada M, Yamamori S, Kishimoto H, Nakayama M, Tanaka Y, Matsuoka K, Takahashi T, Noguchi M, Masumoto K, Utsunomiya T, Kouzan H, Komatsu Y, Ohashi H, Kurosawa K, Kosaki K *et al* (2008) Deletions and epimutations affecting

the human 14q32.2 imprinted region in individuals with paternal and maternal upd(14)-like phenotypes. *Nat Genet* 40: 237 – 242

Kameswaran V, Bramswig NC, McKenna LB, Penn M, Schug J, Hand NJ, Chen Y, Choi I, Vourekas A, Won KJ, Liu C, Vivek K, Naji A, Friedman JR, Kaestner KH (2014) Epigenetic regulation of the DLK1-MEG3 microRNA cluster in human type 2 diabetic islets. *Cell Metab* 19: 135 – 145

Kaneko-Ishino T, Kohda T, Ishino F (2003) The regulation and biological significance of genomic imprinting in mammals. *J Biochem* 133: 699 – 711

Labialle S, Cavaille J (2011) Do repeated arrays of regulatory small-RNA genes elicit genomic imprinting?: Concurrent emergence of large clusters of small non-coding RNAs and genomic imprinting at four evolutionarily distinct eutherian chromosomal loci. *Bioessays* 33: 565 – 573

Labialle S, Vitali P, Cavaille J (2011) Imprinted Small Non-coding RNA Genes: Time to Decipher their Physiological Functions. In *Non Coding RNAs and Epigenetic Regulation of Gene Expression- Drivers of Natural Selection*, Morris KV (ed.), pp. 47 – 75. Norfolk, UK: Caister Academic Press.

Leung AK, Sharp PA (2010) MicroRNA functions in stress responses. *Mol Cell* 40: 205 – 215

Lewis A, Redrup L (2005) Genetic imprinting: conflict at the Callipyge locus. *Curr Biol* 15: R291 – 294

Lin SP, Youngson N, Takada S, Seitz H, Reik W, Paulsen M, Cavaille J, Ferguson-Smith AC (2003) Asymmetric regulation of imprinting on the maternal and paternal chromosomes at the Dlk1-Gtl2 imprinted cluster on mouse chromosome 12. *Nat Genet* 35: 97 – 102

Liu L, Luo GZ, Yang W, Zhao X, Zheng Q, Lv Z, Li W, Wu HJ, Wang L, Wang XJ, Zhou Q (2010) Activation of the imprinted Dlk1-Dio3 region correlates with pluripotency levels of mouse stem cells. *J Biol Chem* 285: 19483 – 19490

Medeiros LA, Dennis LM, Gill ME, Houbaviy H, Markoulaki S, Fu D, White AC, Kirak O, Sharp PA, Page DC, Jaenisch R (2011) Mir-290-295 deficiency in mice results in partially penetrant embryonic lethality and germ cell defects. *Proc Natl Acad Sci USA* 108: 14163 – 14168

Mendell JT, Olson EN (2012) MicroRNAs in stress signaling and human disease. *Cell* 148: 1172 – 1187

Moore T, Haig D (1991) Genomic imprinting in mammalian development: a parental tug-of-war. *Trends Genet* 7: 45 – 49

Noguer-Dance M, Abu-Amero S, Al-Khtib M, Lefevre A, Coullin P, Moore GE, Cavaille J (2010) The primate-specific microRNA gene cluster (C19MC) is imprinted in the placenta. *Hum Mol Genet* 19: 3566 – 3582

Park CY, Choi YS, McManus MT (2010) Analysis of microRNA knockouts in mice. *Hum Mol Genet* 19: R169 – 175

Park CY, Jeker LT, Carver-Moore K, Oh A, Liu HJ, Cameron R, Richards H, Li Z, Adler D, Yoshinaga Y, Martinez M, Nefadov M, Abbas AK, Weiss A, Lanier LL, de Jong PJ, Bluestone JA, Srivastava D, McManus MT (2012) A resource for the conditional ablation of microRNAs in the mouse. *Cell Rep* 1: 385 – 391

Poethig RS (2009) Small RNAs and developmental timing in plants. *Curr Opin Genet Dev* 19: 374 – 378

Potthoff MJ, Kliewer SA, Mangelsdorf DJ (2012) Endocrine fibroblast growth factors 15/19 and 21: from feast to famine. *Genes Dev* 26: 312 – 324

Rago L, Beattie R, Taylor V, Winter J (2014) miR379-410 cluster miRNAs regulate neurogenesis and neuronal migration by fine-tuning N-cadherin. *EMBO J* 33: 906 – 920

Raj A, Rifkin SA, Andersen E, van Oudenaarden A (2010) Variability in gene expression underlies incomplete penetrance. *Nature* 463: 913 – 918

da Rocha ST, Edwards CA, Ito M, Ogata T, Ferguson-Smith AC (2008) Genomic imprinting at the mammalian Dlk1-Dio3 domain. *Trends Genet* 24: 306 – 316

Schratt GM, Tuebing F, Nigh EA, Kane CG, Sabatini ME, Kiebler M, Greenberg ME (2006) A brain-specific microRNA regulates dendritic spine development. *Nature* 439: 283 – 289

Seitz H, Youngson N, Lin SP, Dalbert S, Paulsen M, Bachellerie JP, Ferguson-Smith AC, Cavaille J (2003) Imprinted microRNA genes transcribed antisense to a reciprocally imprinted retrotransposon-like gene. *Nat Genet* 34: 261 – 262

Sekita Y, Wagatsuma H, Nakamura K, Ono R, Kagami M, Wakisaka N, Hino T, Suzuki-Migishima R, Kohda T, Ogura A, Ogata T, Yokoyama M, Kaneko-Ishino T, Ishino F (2008) Role of retrotransposon-derived imprinted gene, Rtl1, in the feto-maternal interface of mouse placenta. *Nat Genet* 40: 243 – 248

Stadtfeld M, Apostolou E, Akutsu H, Fukuda A, Follett P, Natesan S, Kono T, Shioda T, Hochedlinger K (2010) Aberrant silencing of imprinted genes on chromosome 12qF1 in mouse induced pluripotent stem cells. *Nature* 465: 175 – 181

Thumelin S, Esser V, Charvy D, Kolodziej M, Zammit VA, McGarry D, Girard J, Pegorier JP (1994) Expression of liver carnitine palmitoyltransferase I and II genes during development in the rat. *Biochem J* 300(Pt 2): 583 – 587

Turgeon B, Meloche S (2009) Interpreting neonatal lethal phenotypes in mouse mutants: insights into gene function and human diseases. *Physiol Rev* 89: 1 – 26

Wallace C, Smyth DJ, Maisuria-Armer M, Walker NM, Todd JA, Clayton DG (2010) The imprinted DLK1-MEG3 gene region on chromosome 14q32.2 alters susceptibility to type 1 diabetes. *Nat Genet* 42: 68 – 71

Wang ND, Finegold MJ, Bradley A, Ou CN, Abdelsayed SV, Wilde MD, Taylor LR, Wilson DR, Darlington GJ (1995) Impaired energy homeostasis in C/EBP alpha knockout mice. *Science* 269: 1108 – 1112

Wang Q, Chow J, Hong J, Smith AF, Moreno C, Seaby P, Vrana P, Miri K, Tak J, Chung ED, Mastromonaco G, Caniggia I, Varmuza S (2011) Recent acquisition of imprinting at the rodent Sfmbt2 locus correlates with insertion of a large block of miRNAs. *BMC Genomics* 12: 204

Wilkins JF, Haig D (2003) What good is genomic imprinting: the function of parent-specific gene expression. *Nat Rev Genet* 4: 359 – 368

Wolf JB, Hager R (2006) A maternal-offspring coadaptation theory for the evolution of genomic imprinting. *PLoS Biol* 4: e380

Yubero P, Hondares E, Carmona MC, Rossell M, Gonzalez FJ, Iglesias R, Giralt M, Villarroya F (2004) The developmental regulation of peroxisome proliferator-activated receptor-gamma coactivator-1alpha expression in the liver is partially dissociated from the control of gluconeogenesis and lipid catabolism. *Endocrinology* 145: 4268 – 4277

Zhang Y, Hagedorn CH, Wang L (2011) Role of nuclear receptor SHP in metabolism and cancer. *Biochim Biophys Acta* 1812: 893 – 908

